Carbohydrate Research 415 (2015) 54–59

Contents lists available at ScienceDirect

Carbohydrate Research

journal homepage: www.elsevier.com/locate/carres

Understanding reactivity and regioselectivity in Diels–Alder reactions of a sugar-derived dienophile bearing two competing EWGs. An experimental and computational study

Germán F. Giri, Ariel M. Sarotti *, Rolando A. Spanevello *

Instituto de Química de Rosario, Facultad de Ciencias Bioquímicas y Farmacéuticas, Universidad Nacional de Rosario—CONICET, Suipacha 531, S2002LRK Rosario, Argentina

ARTICLE INFO

Article history:
Received 25 June 2015
Received in revised form 23 July 2015
Accepted 28 July 2015
Available online 31 July 2015

Keywords:
Reactivity
Regioselectivity
Diels–Alder
4-Cyanolevoglucosenone
DFT

ABSTRACT

The effect of an extra EWG in the reactivity and regioselectivity in Diels–Alder reactions of β-cyanolevoglucosenone and 4 different dienes was studied by a joint computational and experimental study. Conceptual DFT analysis successfully predicted an important enhancement in the reactivity, and correctly anticipated the regioselectivity in the reactions with isoprene. However, this static treatment failed when dealing the regiochemical preference of the reactions involving a substituted anthracene as diene. MPW1K/6-31G* calculations correctly reproduced the experimental observations. Based on the collected data, we found that when dealing with dienes and dienophiles with no clear electronically activated position, the ease of pyramidalization of the interacting atoms dictates the regioselectivity of the DA reaction.

1. Introduction

The Diels–Alder reaction has been widely applied to the total syntheses of natural products. The reaction itself has become a valuable tool in the development of synthetic, mechanistic, and theoretical concepts, and this important role could be attributed to its remarkable regio- and stereoselectivities.[1] This versatility provides a powerful mean to challenge the construction of complex molecules.[2]

As part of our studies devoted to the pyrolytic conversion of biomass into useful chemicals,[3] we have extensively explored the remarkable dienophilic character of levoglucosenone (1,6-anhydro-3,4-dideoxy-β-D-*glycero*-hex-3-enopyranos-2-ulose) (**1**) (Scheme 1) as chiral building block for the development of new methods for asymmetric synthesis.[4]

In this regard, we recently came across a regiochemical uncertainty found in the literature when comparing the results of the Diels–Alder reaction between levoglucosenone and isoprene which were reported to afford the *meta* regioisomer[5] and the results obtained by Isobe with 3-bromolevoglucosenone and the same diene

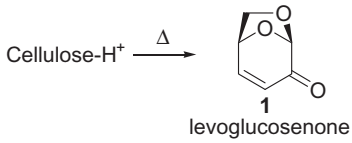

Scheme 1. Preparation of levoglucosenone.

to yield the expected *para* adduct as a key intermediate in the total synthesis of optically active (–)-tetrodotoxin,[6] a formidable complex molecule responsible for the deadly toxicity of the delicious pufferfish (tora fugu). Based on conceptual DFT calculations we concluded that both reactions should display the same regioselectivity, result that was further experimentally validated.[7] Conceptual DFT has emerged as an alternative to the classic frontier molecular orbital (FMO) theory treatment to provide insight into reactivity and selectivity of DA and related cycloaddition reactions.[8] This branch of the density functional theory built the idea that the electron density from molecules in their ground state geometries can be used to quantify fundamental properties (such as electronic chemical potential μ, chemical hardness η, and global electrophilicity ω, that in turn allows the prediction and interpretation of experimental and theoretical data.[9]

Recently, we found that such static treatment failed in predicting correctly the reactivity trends observed experimentally when dealing with α-halogenated derivatives of **1** as dienophiles in DA

* Corresponding authors. Instituto de Química de Rosario, Facultad de Ciencias Bioquímicas y Farmacéuticas, Universidad Nacional de Rosario—CONICET, Suipacha 531, S2002LRK Rosario, Argentina. Tel.: +54 341 4370477; fax: +54 341 4370477.
E-mail addresses: sarotti@iquir-conicet.gov.ar (A.M. Sarotti), spanevello@iquir-conicet.gov.ar (R.A. Spanevello).

http://dx.doi.org/10.1016/j.carres.2015.07.017
0008-6215/

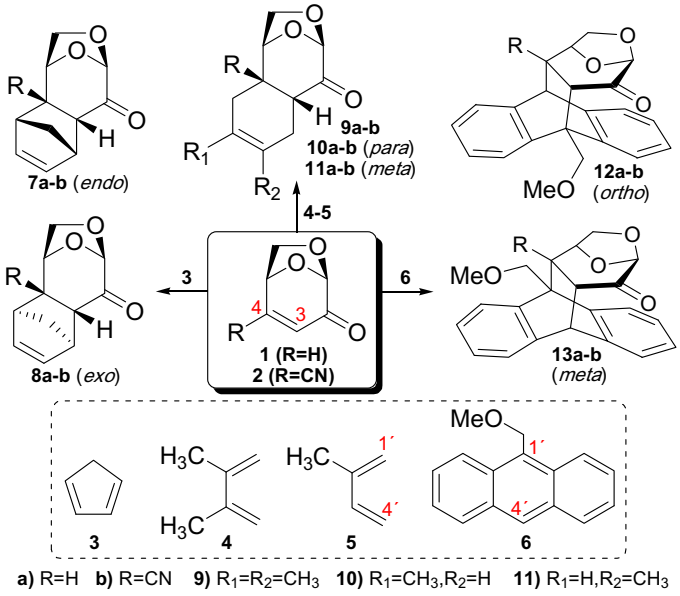

Scheme 2. Diels–Alder reactions between **1** and **2** with **3**–**6**.

reactions with a variety of dienes. Instead, the distortion/interaction model (also known as activation strain model) successfully accounted for the experimental observations.[10] In this fragment approach, the activation energy ($\Delta E^{\ddagger}$) is decomposed as the sum of the distortion energy ($\Delta E_d^{\ddagger}$, energy required to distort the reactants from their initial geometries to their transition state geometries), and the interaction energy $\Delta E_i^{\ddagger}$ (binding energy between the deformed reactants in the transition state).[11] This finding prompted us to combine conceptual DFT analysis and the distortion/interaction model to provide a general understanding of the reactivity trends of polar DA reactions.[12]

In the context of our ongoing interest to synthesize chiral amines from levoglucosenone as novel ligands and catalysts,[13] we have foreseen the introduction of a cyano group at the C4 position of **1**. This structural modification would offer the possibility to create *cis*-fused bicyclic ketones bearing angular cyano group β to the carbonyl, that could subsequently be easily transformed into other useful derivatives, such as 1,4-aminoalcohols.

We speculated that the presence of an exo-cyclic electron withdrawing group (EWG) should increase the reactivity of the dienophile, but would also lead to some ambiguity about which group (i.e. the ketone or the cyano) will have the dominant influence on regio- and stereoselectivity in DA reactions with different dienes. To shed light on these questions, we undertook a conceptual DFT study to predict *in silico* the reactivity and regioselectivity of DA reactions between **2** and four representative dienes: cyclopentadiene (**3**) and 2,3-dimethyl-1,3-butadiene (**4**) as representative cyclic and acyclic symmetric dienes, and isoprene (**5**) and 9-methoxymethyl-anthracene (**6**) as examples of acyclic and cyclic dienes that could lead to regioisomeric adducts (Scheme 2).[14]

2. Results and discussion

First, we computed the global indices of all reagents at the B3LYP/6-31G* level of theory (Table 1). As expected from normal electron demand DA reactions, the electronic chemical potential of **1** and **2** are lower than the μ computed for the dienes **3-6**, indicating that a net charge transfer (CT) will take place from the diene toward the dienophile. As the consequence of the introduction of a second EWG, the electrophilicity of **2** is much higher than that of **1** (ω 3.14 *vs.* 1.83 eV, respectively). This indicates that the former is a much powerful electrophile (defined within the ω scale),[15] increasing the polarity of the DA reaction (as measured by the amount of charge transferred from the diene to the dienophile along the TS).[16] On the other hand, the nucleophilicity of the dienes ranged from 2.94 to 3.91 eV, being **6** the most nucleophilic diene under study.

Table 1
Electronic chemical potential (μ), chemical hardness (η), global electrophilicity (ω) and global nucleophilicity (N) of compounds **1**–**6** computed at the B3LYP/6-31G* level of theory

	μ (au)	η (au)	ω (eV)	N (eV)
1	–0.152	0.172	1.83	2.65
2	–0.186	0.150	3.14	2.02
3	–0.111	0.202	0.83	3.37
4	–0.115	0.222	0.81	2.98
5	–0.121	0.212	0.94	2.94
6	–0.127	0.129	1.69	3.91

It has been proved that the interaction and distortion energies can be fairly predicted as $-\Delta E_i^{\ddagger} = a\omega + bNS + c$ and $\Delta E_d^{\ddagger} = a'NS + b'RS + c'\omega + d'\Delta d + f'$, respectively, where *NS* and *RS* are the number of substituents and ring size of the dienophile, Δd is the predicted asynchronicity at the TS, which in turn can be guessed as $0.39\Delta\omega_k + 0.07$ (*vide infra*) and the coefficients depend on the nature of the diene.[17] Thus, with the static indices shown in Table 1 we could predict that the transition structures arising from the reactions of **3** and **4** with **2** should be both more interacted ($\Delta\Delta E_i^{\ddagger}$ ~4.6 kcal/mol) and distorted ($\Delta\Delta E_d^{\ddagger}$ ~1.8 kcal/mol) than that for **1**. That the interaction prevails over the distortion indicates that the introduction of a cyano group at C4 might increment in at least one order of magnitude the reactivity of the resulting dienophile ($\Delta\Delta E^{\ddagger}$ ~2.8 kcal/mol).

A more challenging task was to predict the influence of the additional EWG in the regioselectivity of the reactions with unsymmetrical dienes (**5** and **6**). For that reason, we next computed the electrophilic Parr and Fukui functions (P_k^+ and f_k^+, respectively) for **1** and **2**, and the nucleophilic Parr and Fukui functions (P_k^- and f_k^-, respectively) for **5** and **6** (Table 2). These local descriptors are useful tools in the study of the regioselectivity in cycloaddition reactions.[18]

Analysis of the P_k^+ of **1** and **2** indicates that C4 is the most electrophilic center in both cases ($\omega_k = \omega P_k^+$), though the difference with C3 is higher in the case of **1** ($\Delta\omega_k = 0.29$ eV *vs.* 0.17 eV). On the other hand, despite C-1′ sites of **5** and **6** are the most nucleophilically activated positions of the dienes, the difference between local nucleophilicity ($N_k = NP_k^-$) between the terminal carbons of the conjugated diene are low ($\Delta N_k = 0.13$ eV for **5** and 0.08 eV for **6**). Similar results were obtained using the condensed Fukui functions for nucleophilic and electrophilic attack (f_k^+ and f_k^-, respectively), indicating that both conceptually different descriptors point in the same

Table 2
Electrophilic, P_k^+, and nucleophilic, P_k^-, Parr functions, condensed Fukui functions for nucleophilic (f_k^+) and electrophilic (f_k^-) attack and 2*pz* HOMO and LUMO coefficients computed for compounds **1**, **2**, **5** and **6** at the B3LYP/6-31G* level of theory

	Site	P_k^+	f_k^+	LUMO *2pz*
1	C3	0.069	0.080	–0.214
	C4	0.463	0.241	0.343
2	C3	0.235	0.123	–0.278
	C4	0.275	0.176	0.314
	Site	P_k^-	f_k^-	HOMO *2pz*
5	C1′	0.529	0.280	0.348
	C4′	0.373	0.237	–0.260
6	C1′	0.308	0.142	0.264
	C4′	0.276	0.121	–0.252

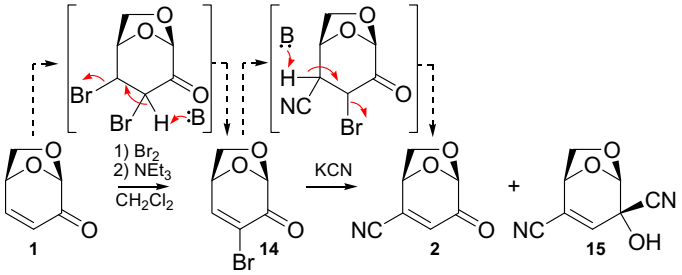

Scheme 3. Synthesis of 4-cyanolevoglucosenone.

direction. According to this analysis, the *para* regioselectivity should be expected for the reaction between **1** or **2** with **5**, and *meta* for the reaction between **1** or **2** with **6**. A similar trend was also found from traditional FMO arguments, by analyzing the HOMO and LUMO coefficients (Table 2).[17,19] In addition, considering that the larger $\Delta\omega_k$ and ΔN_k were computed for **1** and **5**, respectively, the highest and lowest regioselectivities are expected for the **1** + **5** and **2** + **6** reactions, respectively.[16]

However, the known *ortho* preference in the reaction between **1** and **6** suggests additional factors controlling the regioselectivity of these reactions. Thus, the next step was the synthesis of 4-cyanolevolgucosenone (**2**) and its evaluation as dienophile in DA reactions.

The simpler strategy envisioned to achieve our goals was based on the synthesis of the 3-bromolevoglucosenone (**14**) through a bromination/dehydrobromination sequence (Scheme 3). Elimination of the halogen atom bound to C4 takes advantage of the acidity of the ketone's α proton, the use of a non-nucleophilic base render possible the regeneration of the α,β-unsaturated system in one pot reaction leading to **14**. To introduce the cyano group, a similar addition and elimination sequence was thought, but in this case elimination of the bromine atom should start by abstraction of H-4 to rebuild the double bond and extend the conjugation between both electron-withdrawing groups.

As depicted in Scheme 3, reaction of levoglucosenone with bromine in CH_2Cl_2 at 0 °C followed by the addition of Et_3N afforded the 3-bromolevoglucosenone (**14**) in 92% yield. However, the conjugate addition of the cyanide anion to **14** resulted to be more troublesome than expected.

In Table 3 are listed the most representative reaction conditions we used in order to optimize the yields of 4-cyanolevoglucosone.[17] After extensive experimentation, the desired compound **2** could be obtained in moderate yields (up to 42%, entry 4), together with a highly polar byproduct. We were able to isolate and purify that compound which on the basis of the recorded ^1H and ^{13}C NMR spectra was assigned as **15** (Scheme 2). Though

Table 3
Conjugate addition reactions evaluated for the synthesis of **2** starting from **14**

Entry	Conditions[a]	Time	Yield[b]
1	KCN (1.15 eq), Amberlyst, NEt_3, MeCN	0.5 h	31%
2	KCN (7.1 eq), NEt_3, MeCN	24 h	34%
3	KCN (8.2 eq), NEt_3, MeCN, 0 °C	216 h	4%
4	KCN (3.3 eq), CuCN, NEt_3, MeCN	48 h	42%
5	KCN (5.0 eq), CuCN, $(Bu_4N)CN$, MeCN	96 h	41%
6	KCN (1.5 eq), 18-C-6, MeCN	48 h	33%
7	KCN (3.2 eq), MeOH	2 h	19%
8	KCN (1.2 eq), EtOH	0.25 h	25%
9	KCN (1.1 eq), EtOH	120 h	31%
10	KCN (1.1 eq), H_2O	7 min	40%

[a] Unless otherwise noted, all reactions were carried out at room temperature.
[b] Yield corresponds to isolated compound **2** after column chromatography.

Table 4
Diels–Alder reactions between **1** and **2** with **3**–**6**

Entry	Enone	Diene	Conditions	Yield (%)[a]	Selectivity
1	**1**	**3**	25 °C, 4 d	72	95:5[b]
2	**2**	**3**	25 °C, 2 h	85	94:6[b]
3	**1**	**4**	150 °C, 2 h	84	–
4	**2**	**4**	150 °C, 10 min.	79	–
5	**1**	**5**	150 °C, 3 h	73	65:35[c]
6	**2**	**5**	150 °C, 20 min.	68	48:52[c]
7	**1**	**6**	110 °C, 7 d	63	80:20[d]
8	**2**	**6**	110 °C, 1.5 d	77	30:70[d]

[a] Yield corresponds to isolated compounds after column chromatography.
[b] *endo/exo.*
[c] *para/meta.*
[d] *ortho/meta.*

not unexpected, the formation of cyanohydrin **15** by a second nucleophilic addition of the cyanide anion to the carbonyl group could not be suppressed. Nevertheless, using the experimental conditions listed in entry 10 we could obtain sufficient amounts of **2** using a fast, simple and economic procedure with reasonable yields.

With the desired β-cyanoenone in hand, we next evaluated experimentally its performance as dienophile in the DA reactions depicted in Scheme 2. In Table 4 are summarized the results, along with the previously reported for **1** for comparative purposes.[4,10]

In excellent agreement with our conceptual DFT analysis performed, a significant increase in the reaction rates (up to 50-fold) was achieved with **2**. From comparison of entries 1 and 2, it is clear that the ketone group at C2 seems to control the *endo*/*exo* ratio, which was unaffected upon introduction of an exo-cyclic EWG group at C4. Interestingly, such structural modification lead to a modest and high *meta* selectivity when reacting with dienes **5** and **6**, respectively, in clear contrast with the *para* and *ortho* regioselectivities, respectively, observed with **1** at similar reaction conditions. At this point, the regioselectivity prediction with static local indices (and classic FMO arguments) was correct only in the case of isoprene (good *para* selectivity for **1**, lower ratios for **2**). However, the conceptual DFT forecast turned out to be wrong when using **6** as diene. The good *ortho* selectivity experimentally observed in the **1** + **6** reaction, and in particular the clear inversion in the regiochemical preference in the **2** + **6** cycloaddition, motivated us to explore the origins of such findings by analyzing the geometries and energetics of the corresponding transition structures.

A complete exploration of the reaction surfaces was performed using the gradient-corrected MPW1K (Perdew–Wang 1-parameter for kinetics) coupled with the 6-31G* basis set.[20] This functional was developed to provide good accuracy in barrier height prediction, affording accurate results in DA reactions.[21] The most stable TSs located for each channel of addition are shown in Fig. 1.[17,22]

The calculated activation barriers correlated well with the experimental observations. Considering the lowest-energy path for each diene–dienophile system, the $\Delta E^{\ddagger}$ computed for the DA reactions of **2** are lower (2.2–2.9 kcal/mol) than those computed for **1**. It is important to point out that the energy barriers were computed from the global minima conformations of all reagents (*s-trans* in the case of **4** and **5**). In line with the conceptual DFT analysis, the charge transfer computed for **TS-2** (~0.23e) are ca. 1.6 times higher than that computed for **TS-1** (~0.14e) leading to higher interacted TSs in the former ($\Delta\Delta E_i^{\ddagger}$ 3.2–6.4 kcal/mol). On the other hand, the extra substituent in **2** affords more distorted TSs (**TS-2**) than their **TS-1** analogs ($\Delta\Delta E_d^{\ddagger}$ 1.4–2.8 kcal/mol). As a result, the additional stabilization caused by the advanced ionicity of the process due to the introduction of a cyano group at C-3 prevails over the extra strain energy obtained as consequence, leading to lower activation barriers.[12] In line with the experimental findings, the *endo* selectivity was unaffected upon the introduction of an exocyclic EWG group. The

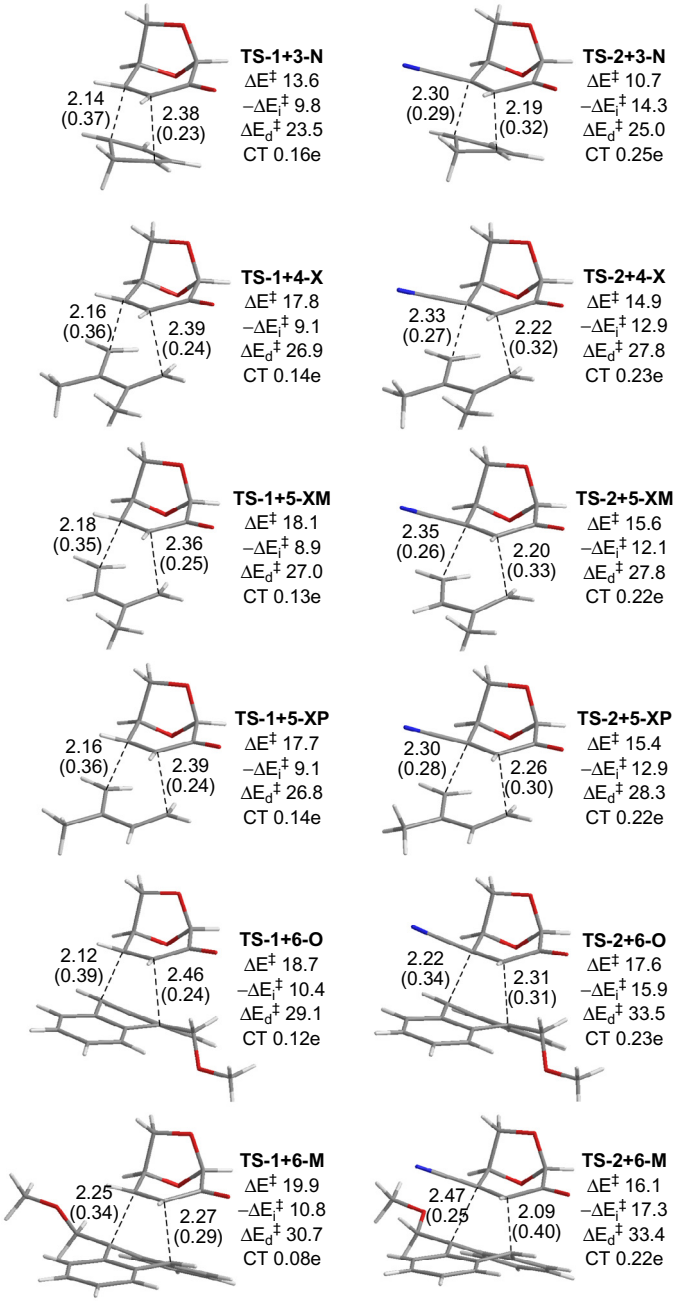

Fig. 1. MPW1K/6-31G* optimized geometries for the TSs of the DA reactions of enones **1**–**2** with dienes **3**–**6**. Selected distances (in Å), Wiberg bond indices (in parentheses), charge transfer (CT) are also shown. Computed activation, interaction and distortion energies are given in kcal/mol.

calculated *endo*/*exo* selectivity for the **1** + **3** and **2** + **3** reactions are 86:14 and 92:8, close to the 95:5 and 94:6 ratios experimentally found, respectively. Regarding the regioselectivity, our calculations reflected good agreement with the experiments. The calculated *para*/*meta* ratios for the reactions of **1** and **2** with **5** are 63:37 and 51:49, respectively, close to the experimentally observed 65:35 and 48:52 ratios, respectively. Similarly, for the reactions involving **6** as diene, the computed 88:12 and 7:93 *ortho*/*meta* ratios agree quite good with the experimental result of 80:20 and 30:70, respectively.

Analysis of the transition structures located for the two symmetric dienes (**3** and **4**) reflects an interesting trend. While in the case of **1** the shorter distances (a higher Wiberg bond indices, WBI) correspond to the bond formation involving the C-4 carbon atom of the dienophile (the most electrophilic center), the bonding between C3/diene is more advanced in the case of **2** (the least electrophilic carbon of the enone).

The higher distortion computed for **TS-2** is associated with the fact that a C—CN bond bends more difficult than a C—H bond out of the plane of the C=C group to which they are attached. This ease of pyramidalization of a CH over a fully substituted sp^2 carbon atom can be seen by measuring the out-of-plane bending angles χ (also known as pyramidalization angles),[12] that were computed as described by Winkler and Dunitz to measure the distortion from planarity of amides.[23] The average χ_{C3} and χ_{C4} in **TS-1** + **3** and **TS-1** + **4** are 19.9° and 32.2°, respectively, whereas in **TS-2** + **3** and **TS-2** + **4** the corresponding angles are higher (χ_{C3} 28.3°) and lower (χ_{C4} 29.5°), respectively, indicating that in **2** the difficulty of pyramidalization at C4 leads to an advanced out-of-plane distortion at C3. The same trend was also found in the case of isoprene (**5**), both in the *para* and *meta* modes of addition. As shown in Fig. 1, **TS-1** + **5-XP** is slightly more asynchronous than **TS-1** + **5-XM** (Δd 0.23Å *vs.* 0.18Å, respectively). The stronger C4—C1 bonding (2.16 Å) in the former arises from the interplay between the most electrophilic carbon of the dienophile and the most nucleophilic carbon of the diene. In contrast, **TS-2** + **5-XM** is more asynchronous than **TS-2** + **5-XP** (Δd 0.15Å *vs.* 0.04 Å, respectively), and the most advanced bonding occurs between C3 and C1′. That the least electrophilic carbon of the dienophile bonds tightly to the most nucleophilic carbon of the diene indicates that the ease of pyramidalization seems to prevail over the electrophilicity in terms of bonding preference. The effect of out-of-plane bending difficulty in controlling the regiochemistry can be best appreciated in the case of DA reactions with 9-methoxymethylanthracene (**6**) as the diene because the terminal carbons of the conjugated diene (a) display nearly the same nucleophilicity, and (b) display different ease of pyramidalization (one of them is a CH and the other a fully substituted sp^2 carbon atom). **TS-1** + **6-O** is much more asynchronous than **TS-1** + **6-M** (Δd 0.34 Å *vs.* 0.02 Å), with the most advanced bonding between C4 and C4′ (the most electrophilic carbon of the diene and the easiest pyramidalized carbon of the dienophile). This tendency is evidenced in **TS-2** + **6-M**, in which the bonding between the least electrophilic carbon of the dienophile and the least nucleophilic carbon of the diene is highly advanced (2.09 Å), whereas the bonding between the most electronically activated carbons (C4 and C1′) is only emerging (2.47 Å). Clearly, the bonding preference of the easily pyramidalized carbons (CH) of both diene and dienophile governs the regiochemistry of the reaction.

3. Conclusion

In summary, the effect of a β-cyano substitution in the dienophilic performance of the corresponding enone was understood by a joint computational and experimental study. Conceptual DFT analysis successfully predicted an important enhancement in the reactivity, and correctly anticipated the regioselectivity in the reactions with isoprene. However, this static treatment failed when dealing the regiochemical preference of the reactions involving a substituted anthracene as diene. MPW1K/6-31G* calculations correctly reproduced the experimental observations. Based on the collected data, we found that when dealing with dienes and dienophiles with no clear electronically activated position, the ease of pyramidalization of the interacting atoms dictates the regioselectivity of the DA reaction.

4. Computational details

All DFT calculations were performed using Gaussian 09.[24] Density functional theory (DFT) calculations were carried out with the B3LYP[25] and the MPW1K[20] functionals, with the 6-31G* basis set.

Geometries for all structures were fully optimized and normal coordinate analyses were used to confirm the nature of the stationary points. All transition structures were confirmed to have only one imaginary frequency corresponding to the formation of the expected bonds. Intrinsic Reaction Coordinate (IRC) calculations were performed to determine the connections between stationary points. The electronic structures of TSs and ground states were analyzed in terms of the Wiberg bond indices (WBI) and the natural charges obtained from the Natural Bond Orbital (NBO) program as implemented in Gaussian 09.[26] Reported thermochemical properties include zero-point energies (ZPEs) without scaling and were calculated at 1 atm and 298.15 K. Free energies in solution were computed on the structures optimized in the gas phase at the MPW1K/6-31G* level of theory with the Polarizable Continuum Model (PCM) as implemented in Gaussian 09 using dichloromethane as the solvent.[27] Distortion energies were computed by performing a single point energy calculation using MPW1K/6-31G* on each of the separated, distorted fragments. The *para*/*meta* and *endo*/*exo* ratios were computed using Boltzmann factors based on activation free energies of all competing TSs. The global electrophilicity index, ω, which measures the energy stabilization when the system acquires an additional electronic charge ΔN from the environment,[28] has been given by the following expression, $\omega = \mu^2/2\eta$, in terms of the electronic chemical potential μ and the chemical hardness η. Both quantities may be approached in terms of the one-electron energies for the frontier molecular orbitals HOMO and LUMO, ε_H and ε_L, as $\mu \approx (\varepsilon_H + \varepsilon_L)/2$ and $\eta \approx (\varepsilon_L - \varepsilon_H)$, respectively.[29] The nucleophilicity index, N, was computed as $N = E_{HOMO(diene)} - E_{HOMO(TCE)}$ (eV),[30] where TCE accounts for tetracyanoethylene. For systems with electron gain, the condensed Fukui index was calculated according to $f_k^+ = q_k(N+1) - q_k(N)$, and for systems with electron donation the consensed Fukui index was calculated according to $f_k^- = q_k(N) - q_k(N-1)$, where $q_k(N+1)$, $q_k(N)$ and $q_k(N-1)$ stand for the gross NBO population on atom k in a molecule with $N+1$, N, and $N-1$ electrons, respectively.[31] The electrophilic Parr function of atom k was computed using the Mulliken atomic spin density (ASD) computed by single-point UB3LYP/6-31G* level of the anion resulting from adding one electron to the optimized neutral B3LYP/6-31G* geometry.[18] The nucleophilic Parr function of atom k was computed using the Mulliken atomic spin density (ASD) computed by single-point UB3LYP/6-31G* level of the cation resulting from removing one electron to the optimized neutral B3LYP/6-31G* geometry.[18]

5. Experimental

Microwave heating was performed in a CEM Discover® System using septum-sealed 10 mL vials for high-pressure reaction conditions with stirring and IR-monitored temperature control. All reagents and solvents were used directly as purchased or purified according to standard procedures. Analytical thin layer chromatography was carried out using commercial silica gel plates (Merck, Silica Gel 60 F254) and visualization was effected with short wavelength UV light (254 nm) and a p-anysaldehyde solution (2.5 mL of p-anysaldehyde + 2.5 mL of H_2SO_4 + 0.25 mL of AcOH + 95 mL of EtOH) with subsequent heating. Column chromatography was performed with silica gel 60 H (Merck), slurry packed, run under low pressure of nitrogen. NMR spectra were recorded at 300 MHz for ^{1}H, and 75 MHz for ^{13}C on a Bruker Avance-300 DPX spectrometer with $CDCl_3$ as solvent and $(CH_3)_4Si$ (^{1}H) or $CDCl_3$ (^{13}C, 76.9 ppm) as internal standards. Chemical shifts are reported in delta (δ) units in parts per million (ppm) and splitting patterns are designated as s, singlet; d, doublet; t, triplet; q, quartet; m, multiplet and br, broad. Coupling constants are recorded in Hertz (Hz). Isomeric ratios were determined by ^{1}H NMR analysis. The structures of the products were determined by a combination of spectroscopic methods such as IR, 1D and 2D NMR (including NOE, DEPT, COSY, HSQC and HMBC experiments) and HRMS. Infrared spectra were recorded on a Shimadzu IR Prestige-21 spectrometer using sodium chloride plate pellets. Absorbance frequencies are recorded in reciprocal centimeters (cm^{-1}). High resolution mass spectra (HRMS) were obtained on a Bruker micrOTOF-Q II LC–MS spectrometer. Optical rotations were determined using a JASCO DIP-1000 digital polarimeter in 100 mm cells and the sodium D line (589 nm) at room temperature in the solvent and concentration indicated. Levoglucosenone (**1**) was synthesized following the procedure developed in our research group.[3]

4-Cyanolevoglucosenone (2): Levoglucosenone (0.86 g, 6.86 mmol) was dissolved in dichloromethane (17 mL) and placed on an ice bath. Then Br_2 was added dropwise (approximately 150 μL) until the solution turned red indicating excess of Br_2. Following this, Et_3N (1.4 mL) was added and let the mixture reacts for 30 minutes. The reaction mix was diluted with water (20 mL) and extracted several times with 15 mL portions of CH_2Cl_2. The combined organic extracts were dried (Na_2SO_4) and concentrated. The residue was purified by flash chromatography to give 3-bromolevoglucosenone (**7**) (1.30 g, 1.91 mmol, 92%), that served as the starting material for the next step. **7** (0.32 g, 1.56 mmol) was vigorously stirred in distilled water (15 mL). When complete dissolution was achieved, KCN (120.4 mg, 1.80 mmol) was added to the solution. After 7 minutes of the last addition, the reaction mixture was extracted several times with 15 mL portions of CH_2Cl_2. The combined organic extracts were dried (Na_2SO_4) and concentrated. The residue was purified by column chromatography to obtain **2** (93.8 mg, 0.62 mmol, 40%). **2**: Yellow solid; mp: 71–72 °C (diethyl ether); $[\alpha]_D = -410.0$ (*c* 1.12, $CHCl_3$); IR (KBr) ν_{max}: 2995, 2371, 2234, 1717 (CO), 1308, 1101, 1055, 970, 893, 731, 621, 559 cm^{-1}; ^{1}H NMR (300 MHz, $CDCl_3$), δ: 6.47 (d, J = 1.5 Hz, 1H, H-3); 5.43 (d, J = 1.5 Hz, 1H, H-1); 5.11 (d, J = 4.3 Hz, 1H, H-5); 4.03–3.94 (m, 2H, H-6*endo*, H-6*exo*); ^{13}C NMR (300 MHz, $CDCl_3$), δ: 185.3 (C, C-2); 136.5 (C, C-5); 131.0 (C, C-4); 113.6 (C, C-7); 100.9 (C, C-1); 73.1 (C, C-5); 67.5 (C, C-6). HRMS: $C_7H_5NO_3Na$ [M + Na^+]: calc.: 174.0167. Found: 174.0172.

Diels–Alder adducts between 1 and 2 with different dienes. *General Procedure*: To an oven-dried 10 mL pressure-rated reaction vial equipped with a stirring bar were added the corresponding enone (0.3–0.5 mmol), dry CH_2Cl_2 (0.7–1 mL) and the corresponding diene (5–10 equiv.) under argon atmosphere. The resulting reaction mixture was stirred at the temperature and time indicated in Table 4 until complete conversion of the enone. The solvent was removed under reduced pressure, and the crude was purified by column chromatography (Hex/AcOEt).

Adduct **7b**: Colorless solid; m.p.: 112–113 °C (ethyl ether); $[\alpha]_D = -173.0$ (*c* 0.81; $CHCl_3$); IR (KBr),$\nu_{máx}$: 2968, 2880, 2230, 1734 (CO), 1335, 1123, 1109, 978, 908, 839, 677 cm^{-1}; ^{1}H NMR ($CDCl_3$, 300 MHz,), δ(ppm): 6.27 (dd, J = 5.7 Hz, J = 3.0 Hz, 1H, H-9), 6.13 (dd, J = 5.7 Hz, J = 3.0 Hz, 1H, H-8), 4.86 (s, 1H, H-1); 4.69 (d, J = 4.5 Hz, 1H, H-5), 4.52 (d, J = 8.4 Hz, 1H, H-6*endo*); 3.89 (dd, J = 8.4 Hz, J = 4.5 Hz, 1H, H-6*exo*), 3.55 (s, 1H, H-7), 3.42 (s, 1H, H-10), 3.26 (d, J = 4.2 Hz, 1H, H-3), 1.90 (d, J = 9.6 Hz, 1H, H-11a), 1.68 (d, J = 9.6 Hz, 1H, H-11b); ^{13}C NMR ($CDCl_3$, 75.5 MHz) δ(ppm): 195.5 (C, C-2), 137.7 (CH, C-8), 133.6 (CH, C-9), 122.4 (C, C-12), 98.7 (CH, C-1), 74.7 (CH, C-5), 68.5 (CH_2, C-6), 53.6 (CH, C-10), 53.0 (CH, C-3), 49, 4 (CH_2, C-11), 48.0 (CH, C-7), 43.9 (C, C-4); HRMS: $C_{12}H_{11}NNaO_3$. Calc.: $[M + Na]^+$ 240.0637. Found: $[M + Na]^+$ 240.0642.

Adduct **9b**: Brown oil; $[\alpha]_D = +2.6$ (*c* 1.00; $CHCl_3$); IR (Film), $\nu_{máx}$: 2913, 2237, 1790, 1746 (CO), 1447, 1115, 957, 907 cm^{-1}; ^{1}H NMR (300 MHz, $CDCl_3$), δ (ppm): 5.16 (s, 1H, H-1), 4.57 (d, J = 4.9 Hz, 1H, H-5), 4.54 (d, J = 8.6 Hz, 1H, H-6*endo*), 4.14 (dd, J = 8.7 Hz, J = 4.8 Hz, 1H, H-6*exo*), 3.26 (d, J = 7.6 Hz, 1H, H-3), 2.77 (d, J = 17.6 Hz, 1H, H-10), 2.63 (d, J = 18.0 Hz, 1H, H-7), 2.28–2.15 (m, 2H, H-7, H-10), 1.70 (s, 1H, H-11), 1.64 (s, 1H, H-12); ^{13}C NMR (300 MHz, $CDCl_3$), δ (ppm): 196.7 (C, C-2), 123.5 (C, C-9), 120.4 (C, C-8), 120.0 (C, C-11), 101.2 (CH, C-1), 77.2 (CH, C-5), 66.3 (CH_2, C-6), 43.1 (C, C-4), 41.7 (CH, C-3),

34.1 (CH_2, C-10), 25.2 (CH_2, C-7), 18.9 (CH_3, C-8a), 18.7 (CH_3, C-9a); HRMS: $C_{14}H_{15}NNaO_3$. Calc.: $[M + Na]^+$ 268.0950. Found: $[M + Na]^+$ 268.0944.

Adducts **10b** and **11b**: Colorless oil; IR (film) $\nu_{máx}$ (cm^{-1}): 2970, 2911, 2356, 2239, 1788, 1744, 1721, 1445, 1117, 1101, 968, 889; ^1H NMR ($CDCl_3$), δ (ppm): 5.47 (broad s, 1H, H-9 of **11b**), 5.34 (broad s, 1H, H-8 of **10b**), 5.17 (s, 2H, H-1 of **10b** and **11b**), 4.58-4.53 (m, 4H, H-5 and H-6 *endo* of **10b** and **11b**), 4.17–4.12 (m, 2H, H-6 *endo* of **10b** and **11b**), 3.32 (d, $J = 7.6$ Hz, 1H, H-3 of **11b**), 3.26 (d, $J = 7.6$ Hz, 1H, H-3 of **10b**), 2.76–2.60 (m, 4H, H-7 of **10b**, H-7 of **11b**, H-10 of **10b**, H-10 of **10**), 2.37-2.16 (m, 4H, H-7 of **10b**, H-7 of **11b**, H-10 of **10b**, H-10 of **11b**)]*, 1.74 (s, 3H, H-8a of **11b**), 1.69 (s, 3H, H-9a of **10b**); ^{13}C NMR ($CDCl_3$), δ (ppm): 196.6 (2C, C-2 of **10b** and **11b**), 131.8 (C, C-9 of **10b**), 128.5 (C, C-8 of **11b**), 119.9 (C, CN of **10b**), 119.8 (C, CN of **11b**), 118.3 (CH, C-9 of **11b**), 115.4 (CH, C-8 of **10b**), 101.3 (CH, C-1 of **10b**), 101.2 (CH, C-1 of **11b**), 76.7 (2CH, C-5 of **10b** and **11b**), 66.3 ($2CH_2$, C-6 of **10b** and **11b**), 43.0 (C, C-4 of **10b**), 42.2 (C,C-4 of **11b**), 41.8 (CH, C-3 of **11b**), 40.7 (CH, C-3 of **10b**), 32.7 (CH_2, C-10 of **10b**), 28.5 (CH_2, C-10 of **11b**), 23.6 (CH_2, C-7 of **11b**), 23.2 (CH_3, C-9a of **10b**), 23.1 (CH_3, C-8a of **11b**), 19.3 (CH_2, C-7 of **10b**); HRMS: $C_{13}H_{13}NNaO_3$. Calc.: $[M + Na]^+$ 254.0793. Found: $[M + Na]^+$ 254.0799.

Adducts **12b** and **13b**: Pale yellow solid; IR (film) $\nu_{máx}$: 2922, 2363, 2236, 1736 (CO), 1670, 1460, 1117, 980, 914, 733 cm^{-1}; ^1H NMR ($CDCl_3$, 300 MHz), δ (ppm): 7.59–7.01 (m, 16 H, arom of **12b** and **13b**), 5.47 (d, $J = 5.4$ Hz, 1H, H-5 of **12b**), 4.88–4.78 (m, 4H, H-3a of **13b**, H-5 of **12b**, H-7 of **13b**), 4.66-4.54 (m, 5H, H-1 of **12b**, H-4a of **12b**, H-7 of **12b**, H-1 of **13b**,), 4.40–4.35 (m, 2H, H-6 *endo* of **12b** and **13b**), 3.95–3.90 (dd, $J = 8.7$ Hz, $J = 5.5$ Hz, 1H, H-6 *exo* of **13b**), 3.88–3.84 (dd, $J = 8.7$ Hz, $J = 5.5$ Hz, 1H, H-6 *exo* of **12b**), 3.75 (s, 3H, H-8 of **13b**), 3.69 (s, 3H, H-8 of **12b**), 3.34 (broad s, 1H, H-3 of **12b**), 3.21 (d, $J = 3.5$ Hz, 1H, H-3 of **13b**); ^{13}C NMR ($CDCl_3$, 75.5 MHz), δ: 195.1 (C, C-2 of **12b** and **13b**), 141.5 (C, arom of **13b**), 141.4 (C, arom of **12b**), 141.0 (C, arom of **12b**), 140.7 (C, arom of **13b**), 140.5 (C, arom of **13b**), 139.6 (C, arom of **12b**), 138.8 (C, arom of **12b**), 138.3 (C, arom of **13b**), 127.5–121.5 (CH, arom of **12b** and **13b**), 120.3 (C, CN of **13b**), 120.2 (C, CN of **12b**), 99.1 (CH, C-1 of **12b**), 99.0 (CH, C-1 of **13b**), 77.8 (CH, C-5 of **12b**), 73.5 (CH, C-5 of **13b**), 71.2 (CH_2, C-7 of **13b**), 69.8 (CH_2, C-7 of **12b**), 67.9 (CH_2, C-6 of **13b**), 67.3 (CH_2, C-6 of **12b**), 59.8 (CH_3, C-8 of **13b**), 59.2 (CH_3, C-8 of **12b**), 53.8 (CH, C-4a of **12b**), 53.4 (CH, C-3 of **13b**), 51.0 (CH, C-3 of **12b**), 50.7 (C, C-4a of **13b**), 50.3 (C, C-3a of **12b**), 48.3 (C, C-4 of **13b**), 46.7 (CH, C-3a of **13b**), 46.0 (C, C-4 of **12b**); HRMS: Calc.: $[M + Na]^+$ 396.1212. Found: $[M + Na]^+$ 396.1197.

Acknowledgements

This research was supported by ANPCyT, CONICET and UNR from Argentina. G. F. G. thanks ANPCyT and CONICET for the award of a fellowship.

Appendix: Supplementary material

Supplementary data to this article can be found online at doi:10.1016/j.carres.2015.07.017.

References

1. Fringuelli F, Taticchi A. The Diels-Alder reaction. New York: Selected Practical Methods John Wiley & Sons, Inc; 2002.
2. Nicolaou KC, Snyder SA, Montagnon T, Vassilikogiannakis G. *Angew Chem Int Ed Engl* 2002;41:1668–98.
3. Sarotti AM, Spanevello RA, Suárez AG. *Green Chem* 2007;9:1137–40.
4. (a) Corne V, Botta MC, Giordano EDV, Giri GF, Llompart DF, Biava HD, et al. *Pure Appl Chem* 2013;85:1683–92; (b) Sarotti AM, Zanardi MM, Spanevello RA, Suárez AG. *Curr Org Synth* 2012;9:439–59; (c) Sarotti AM, Joullié MM, Spanevello RA, Suárez AG. *Org Lett* 2006;8:5561–4.
5. Miftakhov MS, Gaisina IN, Valeev FA. *Russ Chem Bull* 1996;45:1942–4.
6. Nishikawa T, Asai M, Ohyabu N, Yamamoto N, Fukuda Y, Isobe M. *Tetrahedron* 2001;57:3875–83.
7. Sarotti AM, Suárez AG, Spanevello RA. *Tetrahedron Lett* 2011;52:3116–9.
8. Ess DH, Jones GO, Houk KN. *Adv Synth Catal* 2006;348:2337–61.
9. Geerlings P, De Proft F, Langenaeker W. *Chem Rev* 2003;103:1793–873.
10. Sarotti AM, Spanevello RA, Suárez AG. *Tetrahedron Lett* 2011;52:4145–8.
11. van Zeist W-J, Bickelhaupt FM. *Org Biomol Chem* 2010;8:3118–27.
12. Sarotti AM. *Org Biomol Chem* 2014;12:187–99.
13. (a) Sarotti AM, Spanevello RA, Suárez AG, Echeverría GA, Piro OE. *Org Lett* 2012;14:2556–9; (b) Zanardi MM, Botta MC, Suárez AG. *Tetrahedron Lett* 2014;55:5832–5; (c) Zanardi MM, Suárez AG. *Tetrahedron Lett* 2015;56:3762–5.
14. The reactions of these dienes with levoglucosenone have been already studied in our group and this data was used to validate our computational findings. See references. 4c and 10.
15. Domingo LR, Aurell MJ, Perez P, Contreras R. *Tetrahedron* 2002;58:4417–23.
16. Domingo LR, Sáez JA. *Org Biomol Chem* 2009;7:3576–83.
17. For further details in this issue, see Supporting Information.
18. Domingo LR, Pérez P, Sáez JA. *RSC Adv* 2013;3:1486–94.
19. Houk KN. *J Am Chem Soc* 1973;95:4092–4.
20. Lynch BJ, Fast PL, Harris M, Truhlar DG. *J Phys Chem A* 2000;104:4811–5.
21. Jones GO, Guner VA, Houk KN. *J Phys Chem A* 2006;110:1216–24.
22. We have previously studied the DA reactions of 1 with 3-5 at the MPW1K/6–311+G(d,p) level of theory (see reference 10).
23. Winkler FK, Dunitz JD. *J Mol Biol* 1971;59:169–82.
24. Frisch MJ, Trucks GW, Schlegel HB, Scuseria GE, Robb MA, Cheeseman JR, et al. Gaussian 09. Wallingford CT: Gaussian, Inc.; 2009.
25. (a) Lee C, Yang W, Parr RG. *Phys Rev B* 1989;37:785–9; (b) Becke AD. *J Chem Phys* 1993;98:1372–7; (c) Becke AD. *J Chem Phys* 1994;98:5648–52.
26. NBO Version 3.1, Glendening, E. D.; Reed, A. E.; Carpenter, J. E.; Weinhold, F. For some original literature references, see:(a) Reed AE, Weinstock RB, Weinhold F. *J Chem Phys* 1986;83:735–46; (b) Reed AE, Curtiss LA, Weinhold F. *Chem Rev* 1988;88:899–926.
27. For a review on continuum solvation models, see: Tomasi J, Mennucci B, Cammi R. *Chem Rev* 2005;105:2999–3093.
28. Parr RG, von Szentpaly L, Liu S. *J Am Chem Soc* 1999;121:1922–4.
29. (a) Parr RG, Pearson RG. *J Am Chem Soc* 1984;105:7512–6; (b) Parr RG, Yang W. Density Functional Theory of Atoms and Molecules. New York: Oxford University Press; 1989.
30. Domingo LR, Chamorro E, Pérez P. *J Org Chem* 2008;73:4615–24.
31. Yang W, Mortier WJ. *J Am Chem Soc* 1986;108:5708–11.